Available online at www.sciencedirect.com
ScienceDirect
International Journal of Heat and Mass Transfer 51 (2008) 807–822
International Journal of HEAT and MASS TRANSFER
www.elsevier.com/locate/ijhmt

Critical assessment of arterial transport models

Mehrzad Khakpour, Kambiz Vafai *

Mechanical Engineering Department, University of California, Riverside, CA 92521, USA

Received 15 January 2007; received in revised form 21 April 2007
Available online 28 June 2007

Abstract

Works pertinent to arterial transport models are analyzed and a critical assessment of the models utilized in the study of fluid flow and mass transfer within the arteries is presented with an emphasis on the role of porous media. Arterial transport models are assessed and classified based on their ability to physically prescribe the arterial anatomy as well as the related transport processes. Pertinent models such as wall-free, homogeneous-wall, and multi-layer models as well as the governing equations and different types of boundary conditions utilized in each model are analyzed.

1. Introduction

Over the past few decades, the study of causes, genesis, and development of cardiovascular diseases (CVD) has been receiving increasingly more attention. The American Heart Association [1] reports that nearly 80 million American adults (one in three) have one or more types of CVD. Of this population only 47% are estimated to be of age 65 or older. Mortality data show that CVD, as the underlying cause of death, accounted for one out of every 2.8 deaths in the United States. Today, scientists from various fields of study are contributing in achieving a better understanding of the processes involved in CVD. Numerous attempts have been made to apply engineering principles such as transport phenomena to the medical and biological processes. Transport processes are fundamental in various aspects of life sciences. Interactions involving fluid mechanics, heat transfer, and mass transport in biology and medicine are pervasive in understanding the causes of diseases and in the development of new prophylactic, diagnostic, and therapeutic procedures for improving human health. Nearly all the human tissues are categorized as porous media. Thus, fundamentals of transport through porous media have found outstanding applications in biological and biomedical sciences. Advances in numerical simulations and emergence of sophisticated porous transport models have significantly improved the study and analysis of transport in living tissues.

Atherosclerosis, as one of the prevalent CVD, has been studied extensively over the past few decades. It is a progressive disorder of the arterial wall that leads to gradual and uneven narrowing of the arteries through the development of fibrous or fatty plaques within the arterial walls. One of the fundamental causes of the plaque development is believed to be the abnormal enlargement of the intima by infiltration and accumulation of macromolecules such as lipoproteins and the associated cellular and synthetic reactions. Fluid dynamics of blood (hemodynamics) is considered to play a major role in the genesis and development of atherosclerosis. This work presents a critical assessment and analysis of models used in the study of the transport within the arteries with an emphasis on the application of transport through porous media.

In this work, first a brief overview of human blood circulation system, arterial anatomy, and atherosclerosis is presented. Next, the blood rheology and the importance of hemodynamics in the study of atherosclerosis are discussed. Due to porous nature of the arterial wall, the essentials of the models used in analyzing fluid flow and mass transfer through porous media and its role in the study

* Corresponding author. Tel.: +1 951 827 2135; fax: +1 951 827 2899.
E-mail address: vafai@engr.ucr.edu (K. Vafai).

0017-9310/$ - see front matter © 2007 Elsevier Ltd. All rights reserved.
doi:10.1016/j.ijheatmasstransfer.2007.04.021

Nomenclature

C_0	reference species concentration
c	species concentration
c_F	Forchheimer parameter
$\overline{c}$	mean solute concentration
D	mass diffusion coefficient
D_o	overall mass transfer coefficient
D'_e	effective diffusivity per unit length
F	inertia coefficient
J	unit vector oriented along the velocity vector
J_v	transmural velocity
J_s	transmural solute flux
K_p	consistency coefficient (power law model for non-Newtonian fluids)
K_l	solute lag coefficient
K	permeability of the porous medium
K'	permeability per unit length
k	reaction rate coefficient
k_0	lower limit Quemada viscosity constant
k_∞	upper limit Quemada viscosity constant
L_p	hydraulic conductivity
N''_S	absolute molar flux of the solute across the membrane
n_p	power law index (for non-Newtonian fluids)
n	unit vector in wall normal direction
p	pressure
R	radius of the artery
R_u	universal gas constant
Re	Reynolds number
Re_1	$=\max(1, Re)$
Re_K	Reynolds number in a porous medium
Sc	Schmidt number
T	temperature
t	time
U_0	characteristic (reference) velocity
u	velocity in the direction of the flow
u_p	pore velocity
V	Velocity vector

Greek symbols

α	Womersley number
ε	porosity of a medium
ϕ_f	partition coefficient
φ	hematocrit
$\dot{\gamma}$	shear rate
$\dot{\gamma}_0$	reference shear rate
$\dot{\gamma}_c$	a parameter for Quemada model defined by a phenomenological model
λ^*	tortuosity of a medium
μ	dynamic viscosity
μ_0	dynamic viscosity of Plasma
μ_∞	Casson (asymptotic) dynamic viscosity
ν	kinematic viscosity
ν_0	reference kinematic viscosity
π	osmotic pressure
ρ	density
τ_y	fluid yield stress
$\overline{\tau}$	fluid shear stress
σ_d	osmotic reflection coefficient
σ_f	Staverman filtration coefficient
f	frequency
ω_v	angular velocity
$\dot{\omega}$	species source/sink term

Subscripts

e	effective property
w	wall
f	fluid
end	endothelium

Symbols

$\langle\ \rangle$	"local volume average" of a quantity
Δ	differential of a quantity

of transport within biological tissues are analyzed. Finally, a critical review and assessment of the models used in the study of arterial mass transport is presented.

2. Arterial anatomy and development of CVD

The development and function of complex living organs require oxygen and nutrients to be constantly available for the metabolic needs of the cells. This is done via a complex blood circulation system. A schematic of human blood circulation system is shown in Fig. 1. The human body's circulatory system has three distinct parts: the heart (coronary circulation), the lungs (pulmonary circulation), and the rest of the system (systemic circulation). An average human body has roughly 5 liters of blood continuously pumped through the circulatory system delivering nutrients and oxygen, removing waste, and performing other vital tasks.

The blood vessels are part of the circulatory system and function to transport blood throughout the body. The main outlet from the heart, the aorta, branches into several arteries, each serving a particular organ or system. These arteries successively branch into smaller vessels until finally a diffusing system, the capillary bed, is reached. Capillaries are the smallest components of the circulatory system. The structure of the capillaries for each organ is developed in a way to meet its requirements. The blood and the cells exchange substances via selective and specific permeation through two different biomembranes: the cell membrane and the capillary wall. The blood vessels are roughly grouped as venous and arterial, determined by whether

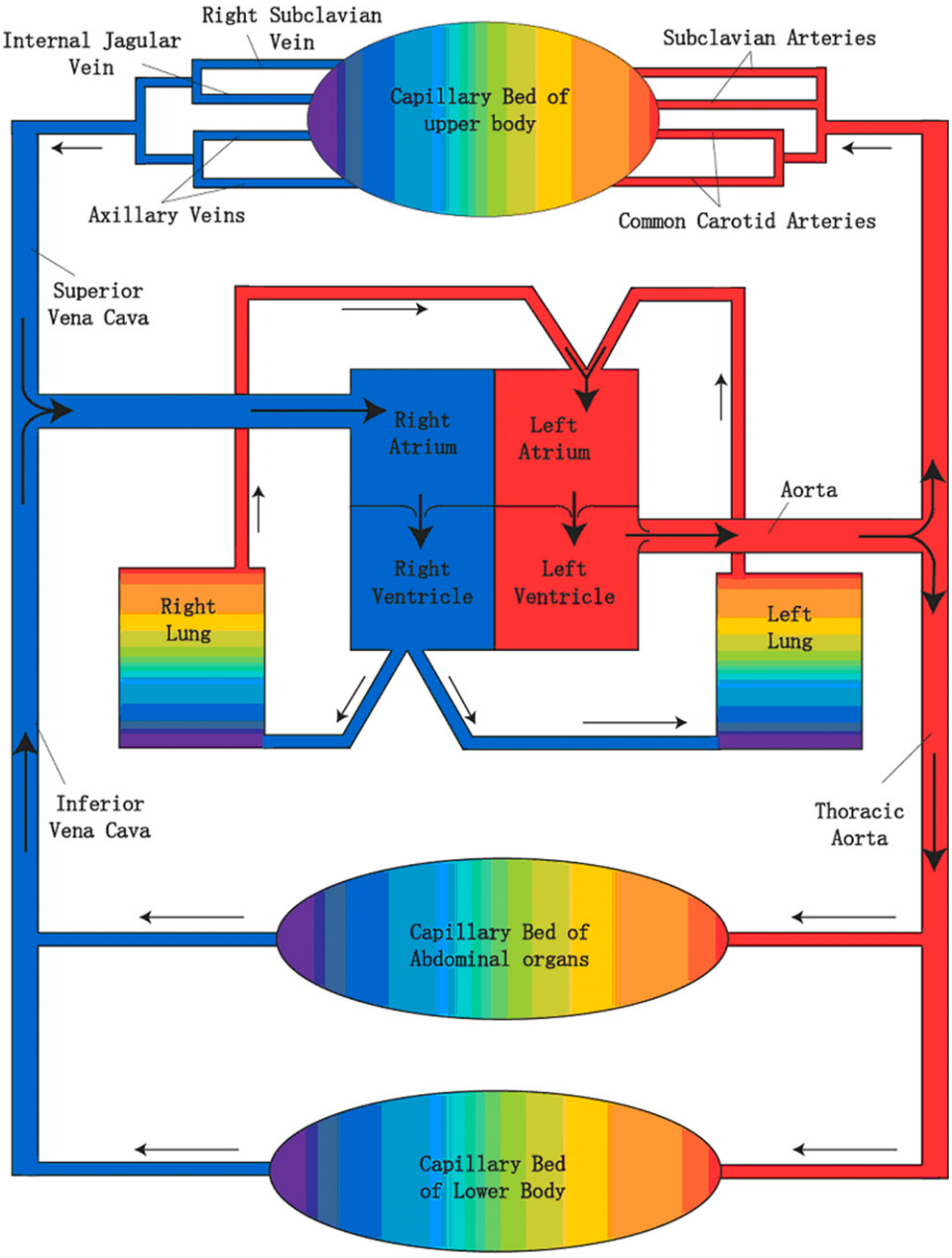

Fig. 1. A schematic of human blood circulation system.

the blood inside them is flowing toward or away from the heart, respectively. The term "arterial blood" and "venous blood" are used to indicate oxygenated and deoxygenated blood, respectively. The exceptions are the pulmonary artery, which carries venous blood and pulmonary vein that contains arterial blood.

A typical anatomical structure of an arterial wall is discussed by Yang and Vafai [2]. Fig. 2 shows a schematic of an arterial wall. Going from the lumen to the most external layer, a large artery is comprised of the following six layers: glycocalyx, endothelium, intima, internal elastic lamina (IEL), media, and adventitia. The luminal glycocalyx is a thin layer of macromolecules which is believed to cover the plasma membrane of a single layer of endothelial cells, and the entrance of the intercellular junctions. Immediately in contact with the glycocalyx is endothelium, a single layer of endothelial cells, which are elongated in the direction of blood flow. Endothelial cells are interconnected through intercellular junctions. Internal elastic lamina is an impermeable elastic tissue with fenestral pores and lies between intima and media. In contrast to the media, which contains alternating layers of smooth muscle cells and elastic connective tissue, the intima is mainly comprised of proteoglycan and collagen fibers. The media layer is surrounded by a loose connective tissue, called the adventitia, which contains some capillaries (lymphatic and vasa vasorum). In larger arteries of certain species the capillaries of the adventitia may penetrate the outer section of the media as well [3].

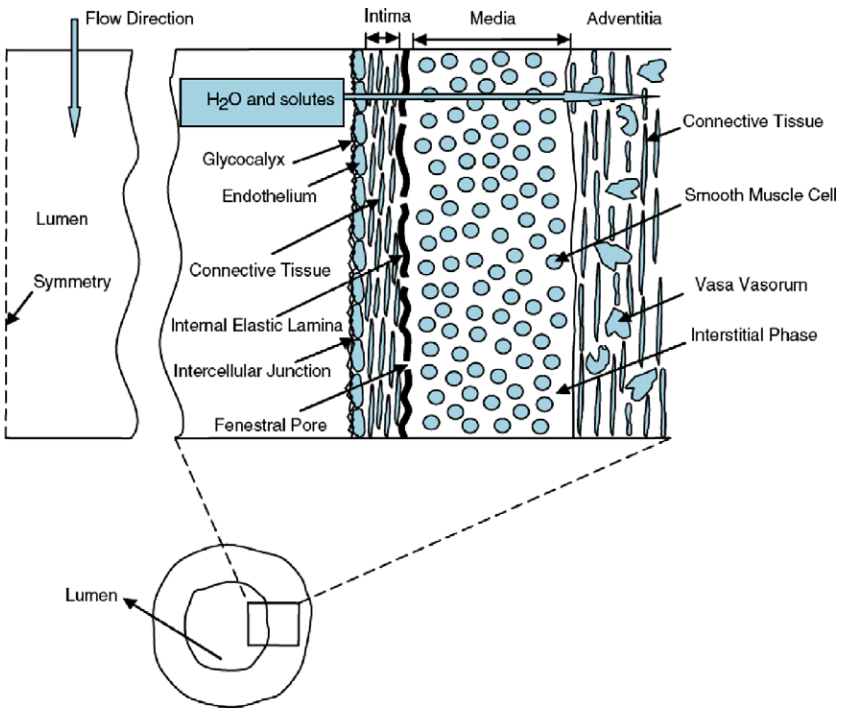

Fig. 2. A schematic of the anatomical structure of an arterial wall [2].

Mass transfer across the arterial wall occurs via two mechanisms: convection associated with pressure-driven transmural flow and mass diffusion caused by concentration gradients. Molecular diffusion is driven by solute concentration gradients within the arterial walls. These gradients are caused by metabolic uptake and production of proteins within tissue cells. Proteins transported from blood through the endothelial and intimal layers usually encounter some mass-transfer resistance. The resistance can be quite high depending on the size and charge of the protein. The proteins can undergo reaction and further penetrate into the media. In addition to the main transport from luminal blood supplies, proteins may also be transported from the adventitia to the media through the vasa vasorum.

Blood vessels are known to differ from each other in both their structural features and biochemical composition of their walls. Major arteries, however, possess similar anatomical structure and properties. Therapeutic solutions can be realized through understanding a range of phenomena including the response of blood vessels under physiological loads. The strength and deformation properties of blood-vessel walls depend on the structure and biochemical composition to a certain extent. Although assumed rigid in some arterial blood flow and mass transport studies, blood vessels are elastic in nature. Vito and Dixon [4] put forth a review of recent blood vessel constitutive models. They provided a comparative overview of four different models along with their corresponding assumptions, limitations, and benefits. These were pseudoelastic, randomly elastic, poroelastic, and viscoelastic models. More information on the mechanics of the arteries was also provided by Vito and Dixon [4].

Various types of CVD can be broadly divided into two categories. First category is related to heart diseases such as heart failure, congenital heart disease, and coronary heart disease and the second category is associated with the blood vessel anomalies and includes atherosclerosis, stroke, thrombosis, and aneurysm. These may have different or common causes and some may lead to the development of another. This work focuses mostly on the processes and mechanisms involved in the second category and specifically atherosclerosis. A brief overview of the causes and development stages of atherosclerosis was presented by Quarteroni et al. [5]. Atherosclerosis is recognized as a focal chronic inflammatory fibroproliferative disease of the inner arterial wall. It is characterized as a progressive disorder, which leads to gradual and uneven narrowing of arteries through the development of fibrous or fatty plaques within the arterial walls. The onset and progression of atherosclerosis involves many processes, however, the fundamental cause of the plaque development is believed to be the abnormal enlargement of the intima by the infiltration and accumulation of macromolecules such as lipoproteins and the associated cellular and synthetic reactions.

The arterial system is tortuous; branches at times to reach an end organ. The cross-sectional area along the axis may enlarge at branch points, sinuses, and aneurysms. If the area diverges, the flow must decelerate, and an adverse pressure gradient develops. In these situations, flow separation is possible and typically occurs along the walls of the sinus. Normal arterial flow is laminar with secondary flows

generated at curves and branches. The arteries are living organs that can adapt to and change with the varying hemodynamic conditions. However, in certain circumstances, unusual hemodynamic conditions create an abnormal biological response. Velocity profile skewing can create pockets in which the direction of the wall shear stress oscillates [6]. Clinical observations indicate that atherosclerotic lesions develop often at branches and bifurcations where disturbed flow patterns are observed [5]. Atherosclerotic disease tends to be localized in these sites and results in a narrowing of the artery lumen (stenosis). A stenosis can cause turbulence and reduce flow by means of viscous head losses and flow choking. Very high shear stresses near the throat of the stenosis can activate platelets and thereby induce thromboembolism, which can totally block blood flow to the heart or brain.

High dependency of the genesis and development of atherosclerosis upon transport processes within the arteries has led scientists to employ advanced tools and sophisticated models to study the hemodynamics and mass transport within the arteries. In what follows, a brief overview of the blood rheology and the role of hemodynamics in the pathogenesis of atherosclerosis is presented.

3. Blood rheology and hemodynamics

From a rheological point of view, blood can be thought of as a solid–liquid suspension, with the cellular elements being the solid phase. Since blood is a two-phase liquid, its fluidity at a given shear rate and temperature is determined by the rheological properties of the plasma and cellular phases and by the hematocrit (defined as the volume fraction of the red cells in the blood) of the cellular phase. Plasma is the liquid phase of the blood. It can be considered as a Newtonian fluid (i.e. viscosity independent of shear rate). The normal range of viscosity for healthy plasma is reported to range from 1.10 to 1.35 cP [7].

For a laminar blood flow, cellular elements act in disturbing the flow streamlines and therefore influencing the blood viscosity [8]. With increasing the amounts of cells, flow lines are progressively disturbed, and viscosity of blood increases as compared to that of plasma. Thus the degree of disturbance of flow streamlines and consequently the viscosity of blood depends mainly on the concentration of the red blood cells, which is represented by the hematocrit. There is an exponential relationship between the hematocrit value and blood viscosity, such that at higher levels of hematocrit, blood viscosity becomes increasingly sensitive to hematocrit alterations [9]. Due to their relatively higher number and volume concentration, red blood cells have a more pronounced role in the rheology of blood in large arteries as compared to white cells and platelets. In particular, the white blood cells have a very low number and volume concentration as compared to red blood cells. In the microcirculation, where blood vessel sizes are comparable to the size of red blood cells, every single red blood cell may have the potential to influence the flow field.

Blood is approximately four times more viscous than water. It does not exhibit a constant viscosity at all flow rates and is especially non-Newtonian in the microcirculatory system. The non-Newtonian behavior of blood is most evident at very low shear rates [10]. There are several constitutive relationships to study the non-Newtonian behavior of blood, i.e. power-law model, Casson model, Quemada model and viscoelastic model. One of the most commonly used constitutive relationships to express viscosity of the blood is the power law model

$$\mu = K_{\mathrm{p}}|\dot{\gamma}|^{n_{\mathrm{p}}-1} \tag{1}$$

where K_{p}, n_{p}, $\dot{\gamma}$ are the consistency coefficient, the power law index, and the shear rate, respectively. The Casson model represents a non-linear relationship between shear stress and shear strain and is given by [11]:

$$\sqrt{\bar{\tau}} = \sqrt{\dot{\gamma}\mu_{\infty}} + \sqrt{\tau_{\mathrm{y}}} \tag{2}$$

where $\bar{\tau}$, τ_{y}, and μ_{∞} denote the fluid shear stress, fluid yield stress and viscosity at high shear rate (Casson viscosity or asymptotic viscosity), respectively. The Quemada model [12] is useful in evaluating the viscosity of concentrated disperse systems based on shear rate and hematocrit. It is given as

$$\mu = \mu_0\left(1 - \frac{\varphi}{2}\left(\frac{k_0 + k_{\infty}\sqrt{\dot{\gamma}/\dot{\gamma}_{\mathrm{c}}}}{1 + \sqrt{\dot{\gamma}/\dot{\gamma}_{\mathrm{c}}}}\right)\right)^{-2} \tag{3}$$

where μ_0 and φ are the plasma viscosity and the hematocrit, respectively. The parameter $\dot{\gamma}_{\mathrm{c}}$ is defined by a phenomenological model. The parameters k_0, and k_{∞} are the lower and upper limit Quemada viscosity constants, respectively. In an investigation of Stokes' second problem for non-Newtonian fluids, Ai and Vafai [13] have studied and compared the effects of reference shear rate on the wall shear stress for different blood models. Reference shear rate is defined as

$$\dot{\gamma}_0 = U_0\sqrt{f/v_0} \tag{4}$$

where U_0, f, and v_0 are the reference velocity, frequency, and the representative viscosity of the Newtonian fluid. Fig. 3 shows the temporal variation of wall shear stress with a reference shear of unity for different constitutive blood viscosity models.

Due to the cyclic nature of the heart pump that creates pulsatile conditions in all arteries, blood flow and pressure are unsteady. The heart ejects blood during systole while it rests during diastole (no blood is ejected). The flow out of the heart is intermittent, going to zero when the aortic valve is closed [6]. A nondimensional frequency parameter, the Womersley number α, governs the relationship between the unsteady and viscous forces and is given by

$$\alpha = R\sqrt{\omega_{\mathrm{v}}/v} \tag{5}$$

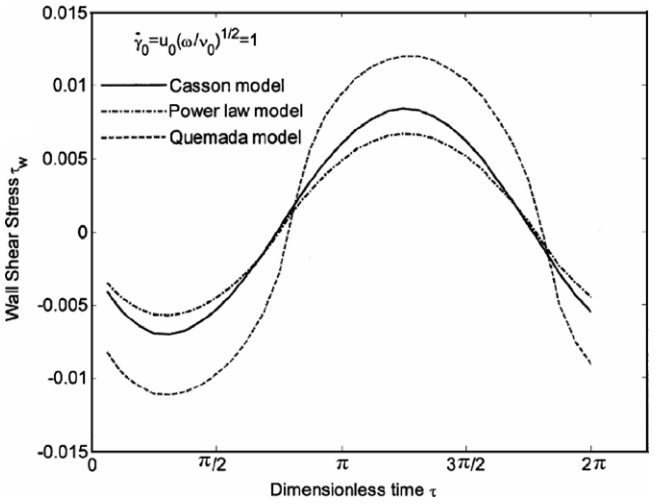

Fig. 3. Temporal variation of wall shear stress with a reference shear of 1.0 [13].

where R is the radius of the artery, ω_v is the angular velocity, and v is the kinematic viscosity. Pulsatile nature of the blood flow in the cardiovascular system has a number of hemodynamical and rheological effects. When flows are changing with time, such as blood flow in the human circulation, the liquid generally demonstrates elastic as well as viscous effects, both of which determine the stress-to-strain rate relationship. Such liquids are called viscoelastic. Blood plasma normally shows viscosity only, while whole blood is both viscous and elastic. The viscoelasticity of blood is traceable to the elastic red blood cells, which occupy roughly 40–50% of the volume.

When the red cells are at rest they tend to aggregate and stack together in a space efficient manner. In order for blood to flow freely, the size of these aggregates must be reduced, which in turn provides some freedom of internal motion. The forces that disaggregate the cells also produce elastic deformation and orientation of the cells, causing elastic energy to be stored in the cellular microstructure of the blood. As flow proceeds, the sliding of the internal cellular structure requires a continuous input of energy, which is dissipated through viscous friction. These effects make blood a viscoelastic fluid [14]. In the framework of large and medium vessels, it is generally agreed that, under physiological conditions, the Newtonian model for blood rheology is acceptable and therefore, in most arteries, blood is taken as a Newtonian fluid with a constant viscosity of 4–6 cP for a normal hematocrit.

Fluid dynamics of blood flow in arteries and the effects of pertinent parameters on the vascular function and the development of CVD have been reviewed in the literature [6,15–23]. As blood flows along the endothelium, a shear stress is generated to retard the flow. The wall shear stress is thus central to the vascular response to hemodynamics. A correlation between fluid dynamic forces and atherosclerotic disease has long been speculated. Over the years, numerous analytical, numerical, and experimental studies have been carried out to illuminate this correlation. The hypothesis was based on the observation that atherosclerotic disease is focal, often occurring at sites of complex hemodynamics such as arterial bifurcations and junctions. It is believed that hemodynamic factors, such as the wall shear stress, particle residence time, recirculation zones, arterial wall strain and wall compliance, play significant roles in the onset and localization of atherosclerosis [16,23]. Since these hemodynamic factors occur at the lumen–endothelium interface, the behavior and dysfunction of endothelial cells is of great importance. Amongst various hemodynamic parameters acting on the endothelium, the wall shear stress and its derivatives are the most influential on the distribution of atherosclerotic lesion.

There are several prevailing hypotheses linking non-uniform hemodynamics with abnormal biological events which are based on the wall-shear stress concept. For example, the high shear stress theory suggests that acute shearing stresses may cause endothelial dysfunction [24–26]; hence, it may be responsible for local plaque formation. On the other hand, the low shear stress theory argues that early atheroma occurs in regions of low wall shear stress [27–29]. Work also points to oscillatory and pulsatile shear stress effects [30–34] as well as the influence of spatial shear stress gradients [35–40].

It has become widely accepted that regions of arterial tree with low or oscillatory shear stress are more likely to develop atherosclerosis [27,30,41]. For instance, the carotid sinus is shown to be a preferential site of lipid deposition [20]. Carotid bifurcation is a site where the main artery in the neck (the common carotid artery) divides to form the external and internal carotid arteries. Carotid sinus is a localized dilation of the internal carotid artery right after branching from the common carotid artery opposite the flow divider. The carotid sinus is characterized by flow recirculation zones, oscillatory levels of wall shear stress, and increased particle residence time [20]. The hemodynamic conditions in such zones may cause a longer cell-to-cell interaction and trans-endothelial transport at the endothelium–lumen interface.

4. Application of porous media in modeling transport through biological tissues

The study of atherogenesis involves both hemodynamics within the arteries and mass transport across the arterial wall. As mentioned earlier, hemodynamical conditions are believed to play an important role in localizing and initiation of atherosclerosis. The study of mass transport across the arterial wall requires knowledge of arterial anatomy as well as sophisticated models to simulate the phenomenon. Arterial wall, like a great majority of other human tissues, can be treated as a porous medium. As such, it is of great importance to characterize the porous media transport models used in describing biological phenomena.

A porous medium is characterized by its porosity represented as the ratio of the void space to the total volume of the medium. Most human tissues can be treated as porous media as they are composed of dispersed cells separated by connective voids where blood flows [42,43]. Earlier studies in fluid flow through porous media have revealed the classical Darcy law which represents a linear relationship between the flow velocity and the pressure gradient across the porous medium:

$$\vec{V} = -\frac{\underline{\underline{\mathrm{K}}}}{\mu}\nabla p \tag{6}$$

where $\underline{\underline{\mathrm{K}}}$ is the permeability tensor, $\vec{V}$ the velocity vector, μ the dynamic viscosity, and ∇p is the pressure gradient. Permeability is a measure of the flow conductivity in the porous medium and is one of the key parameters characterizing a porous medium. Darcy model has been utilized in several biomedical studies [7,44–49].

Although useful, Darcy's law has several substantial shortcomings. It neglects the effects of a boundary or the inertial forces on the fluid flow and heat transfer through porous media [50]. As such, a number of modified models have been proposed. One of these modified models which accounts for the inertial effects is known as Darcy–Forchheimer model. It is given by

$$\nabla p = -\frac{\mu}{K}V + c_{\mathrm{F}}K^{-1/2}\rho|V|V \tag{7}$$

where c_{F} is a dimensionless parameter related to inertial effects. This model is obtained by adding an additional term (Forchheimer term) to account for inertial effects. The transition from Darcy-flow to Darcy–Forchheimer flow depends on the permeability-based Reynolds number. This Reynolds number is defined as

$$Re_K = \frac{u_{\mathrm{p}}\sqrt{K}}{\nu} \tag{8}$$

where u_{p}, K, and ν are the pore velocity, permeability, and kinematic viscosity, respectively. Different transition regions are analyzed by Vafai et al. [51]. Brinkman model takes into account the effect of solid boundaries. It permits the application of no-slip boundary condition along the solid walls that confine the porous medium. Brinkman's model is given by

$$\nabla p = -\frac{\mu}{K}V + \mu_{\mathrm{e}}\nabla^2 V \tag{9}$$

where μ_{e} is the effective viscosity of the porous medium. In the current literature, μ_{e} is often assumed to be equal to μ. For isotropic porous medium, Bear and Bachmat [52] have stated that the effective viscosity is related to the porosity through the following relation:

$$\mu_{\mathrm{e}} = \mu(\lambda^*\varepsilon)^{-1} \tag{10}$$

where ε and λ^* are the porosity and tortuosity of the medium, respectively. Tortuosity is one of the important characteristics of a porous medium and represents the hindrance to flow diffusion imposed by local boundaries or local viscosity. Brinkman's model has been used in a number of biological transport studies [53–55]. In cases where fluid inertia is not negligible, the form drag exerted by the fluid on the solid becomes significant. Vafai and Tien [50] arrived at a generalized model for flow transport through porous media which accounts for various pertinent effects. This generalized model is given by the following equation [50]:

$$\frac{\rho_{\mathrm{f}}}{\varepsilon}\left[\frac{\partial\langle V\rangle}{\partial t} + \langle(V\cdot\nabla)V\rangle\right] = -\nabla\langle P\rangle^f + \frac{\mu}{\varepsilon}\nabla^2\langle V\rangle - \frac{\mu}{K}\langle V\rangle - \frac{\rho_{\mathrm{f}}F\varepsilon}{K^{1/2}}[\langle V\rangle\cdot\langle V\rangle]J \tag{11}$$

where F and ρ_{f} are the dimensionless inertia coefficient and the fluid density, respectively. The parameters $\langle P\rangle^f$ and J are the average pressure inside the fluid and a unit vector oriented along the velocity vector V, respectively. The symbol $\langle\ \rangle$, represents the local volume average of a quantity associated with the fluid. This generalized model also accounts for the convective terms. It is important to utilize this equation in tissue media especially those located near the aortas or in skeletal tissues that have higher perfusion rates. A more limited form of this generalized model is referred to as the Brinkman–Forchheimer–Darcy equation. The treatment of species propagation in a mixture that is flowing through a porous medium is given by [2]

$$\frac{\partial\langle c\rangle}{\partial t} + \langle V\rangle\cdot\nabla\langle c\rangle = D_{\mathrm{e}}\nabla^2\langle c\rangle + \dot{\omega} \tag{12}$$

where c is the species concentration, D_{e} is the effective diffusivity, and $\dot{\omega}$ is the source/sink term accounting for the rate of species generation/consumption per unit time and volume.

5. Mass transport across arterial wall

Mass transport through the arteries has been studied using various experimental, analytical, and computational methods. Extensive experimental investigations related to the mass transfer through the arterial wall have been pursued [55–62]. Some of the challenges met in the experimental works include the suitability of animal models for the human disease condition, the challenge of properly controlling all relevant experimental conditions in animal models, and the difficulty of obtaining measurements with adequate spatial resolution, to name a few. Mathematical and numerical modelings have been successful in handling some of these difficulties. There are three important challenges in modeling the mass transport within the arteries, i.e. accurate geometrical description of the artery, proper set of governing equations, and appropriate choice of boundary conditions.

Several geometrical models of the arterial wall have been proposed in the literature. Based on the description of the arterial wall and the underlying assumptions, Prosi et al. [63] have classified these models as three major types, i.e. wall-free, homogenous-wall, and multi-layer-wall models.

The simplest models are named wall-free models. This model solves for the blood flow in the lumen while accounting for the effects of the arterial wall simply by means of an appropriate set of boundary conditions. As such, the solution is independent of the mass transport processes inside the arterial wall. The values of boundary conditions, for instance the filtration velocity, are usually taken directly from the literature. Because of their simplicity, the wall-free models need a relatively small number of parameters, i.e. the diffusivity in plasma, the overall mass transfer coefficient of the wall with respect to the considered solute and the filtration velocity. Nonetheless, they cannot provide any information on the concentration profiles within the wall. This model is mostly used in the study of hemodynamics and the role of hemodynamical parameters in localizing and the onset of atherosclerosis. This model has been used for the study of the dynamics of different solutes such as oxygen, albumin, and low-density lipoprotein (LDL) [64–67].

Back et al. [64] examined the oxygen transport to multiple non-obstructive plaque regions in the main coronary arteries. They employed numerical simulations to solve for the oxygen convective and diffusive processes in the lumen. They considered actual variations of blood flow rate and the velocity field during the cardiac cycle. The flow field was obtained by solving the Navier–Stokes equation for a pulsatile luminal blood flow. They non-dimensionalized the oxygen concentration using its value at the wall and in the free stream. Rappitsch and Perktold [65] and Rappitsch et al. [66] performed numerical simulation of the blood flow and mass transport in large arteries. They obtained the flow field by solving an unsteady three dimensional incompressible Navier–Stokes equations for a Newtonian fluid. They applied no-slip and constant (zero) cross flow on the walls. Solute (albumin or LDL) transport was modeled by an advection–diffusion equation. They included both constant and shear-dependent wall permeability model in the boundary conditions of the advection–diffusion equation.

Wada and Karino [67] applied these relatively simple models to study the concentration polarization of LDL at the luminal surface of an artery. In their study, they considered a steady blood flow with an advection–diffusion equation representing the LDL transport. They assumed that an arterial wall was rigid and permeable to water and applied a filtration velocity of $V_w = 4 \times 10^{-5}$ mm/s which was previously obtained for the filtration of water through a natural artery. At the arterial wall, they employed a mass conservation boundary condition given by

$$V_w c_w - D \left.\frac{\partial c}{\partial n}\right|_w = D_o c_w \tag{13}$$

where c_w is the concentration of LDL at the luminal surface of the vessel (surface concentration), n is the direction normal to the surface, and D_o is the overall mass transfer coefficient of LDL at the vessel wall.

Second type of the mass transfer models are the homogeneous-wall models. In these models, the arterial wall is present; however, its complex heterogeneous structure is approximated by a simple homogeneous layer. The properties of wall are usually approximate values based on the assumption that the arterial wall is a homogeneous porous medium. Such models represent a reasonable compromise between the complexity of the input data and the accuracy of the results and are functional in cases where the concentration distribution across the arterial wall is not of primary importance. In addition to the study of hemodynamics and its localizing role, the homogenous-wall model can be used as a tool to investigate the interaction between the hemodynamical parameters and the arterial wall, for instance shear-dependent permeability of the endothelium.

Homogeneous-wall models have been used by Ethier and Moore [68] and Stangeby and Ethier [69] to study the concentration of oxygen and LDL within the arterial walls. Stangeby and Ethier [69] modeled the fluid flow within both the lumen and wall of a constricted and axisymmetrically stenosed artery and utilized the resulting flow pattern to study LDL transport from blood to the arterial wall. They coupled luminal blood flow and transmural fluid flow through the solution of Brinkman's model. They prescribed a constant pressure at the adventitial vasa vasorum. In addition, they allowed variations in wall permeability due to the occurrence of plaque. They employed an unsteady Navier–Stokes equation of the form

$$\alpha^2 \frac{\partial u}{\partial t} + Re\, u \cdot \nabla u + Re_1 \nabla p - \nabla^2 u = 0 \tag{14}$$

where α is the Womersley number. The parameters Re and Re_1 are defined as $Re = U_0 R/\nu$ and $Re_1 = \max(1, Re)$, where U_0 and R are the characteristic velocity and the radius of the artery, respectively. They utilized a limited form of the generalized equation given by

$$\alpha^2 \frac{\partial u}{\partial t} + Re\, u \cdot \nabla u + Re_1 \nabla p - \nabla^2 u + \frac{R^2}{K} u = 0 \tag{15}$$

where K the Darcian permeability of the artery. In their study, Stangeby and Ethier [69] employed the following unsteady advection–diffusion equation to solve for the concentration field:

$$\alpha^2 \frac{\partial c}{\partial t} + Re\, u \cdot \nabla c - \frac{1}{Sc} \nabla^2 c = 0 \tag{16}$$

where Sc is the Schmidt number.

Sun et al. [70] studied the effects of wall shear stress on the mass transport from blood to and within the wall of a stenosed artery under steady conditions. They used a homogenous-wall model and developed shear dependent endothelial transport properties for different species (LDL and oxygen). They assumed that LDL transport was influenced by shear-dependent hydraulic conductivity, while shear dependent permeability was applied to oxygen transport. Flow and species transport in the lumen was rep-

resented by Navier–Stokes and advection–diffusion equations. They used Darcy's law to solve for the transmural flow in the arterial wall. In their numerical study, Sun et al. [70] coupled the mass transport within the artery with the transmural flow and solved the following advection–diffusion-reaction equation to obtain the species distribution across the arterial wall

$$\nabla \cdot (-D_w \nabla c_w + K_l c_w u_w) = k_w c_w \tag{17}$$

where c_w is the solute concentration in the arterial wall, D_w is the solute diffusivity in the arterial wall, K_l is the solute lag coefficient, and k_w is the reaction (consumption) rate constant. At the lumen–wall interface, they applied the transmural velocity, J_v, and solute flux, J_s. The solute transfer boundary condition at the lumen–wall interface was given as

$$-D_w \nabla c_w n_w + c_w u_w n_w = J_s \tag{18}$$

where n_w represents the interfacial the unit vector normal to the interface. The transmural velocity and solute flux were obtained from Kedem–Katchalsky equations [71], given by

$$J_v = L_p(\Delta p - \sigma_d \Delta \pi) \tag{19}$$

$$J_s = K_{end}\Delta c + (1 - \sigma_f) J_v \bar{c} \tag{20}$$

where L_p, K_{end}, and $\bar{c}$ are the hydraulic conductivity, solute permeability, and mean solute concentration of endothelium, respectively. The terms Δp, Δc, and $\Delta \pi$ are the pressure differential, the solute concentration difference, and the corresponding osmotic pressure differential across the endothelium, respectively. The parameters σ_f and σ_d are the Staverman filtration and osmotic reflection (which account for the selective permeability of biological membranes to certain solutes) coefficients, respectively. Curry [73] has demonstrated that the Staverman reflection coefficients σ_f and σ_d for the convective transport in the fiber matrix can be expressed as

$$\sigma_d = \sigma_f = (1 - \phi_f)^2 \tag{21}$$

where ϕ_f is the partition coefficient, defined based on the distribution of spaces available to a certain spherical molecule in a random fiber matrix made of infinitely long, stiff rods satisfying the Poisson distribution. In addition, Sun et al. [70] prescribed a constant pressure at the adventitial boundary (outer boundary of the arterial wall).

To date, the most comprehensive model used to characterize the arterial wall is the multi-layer model [74–78,63,2]. This model represents the arterial wall to be composed of several heterogeneous porous layers, i.e. endothelium, intima, IEL and media. The multi-layer model is advantageous over the homogeneous-wall model in that it accounts for the particular characteristics and properties of each porous layer. As mentioned earlier, atherosclerosis is characterized as an abnormal thickening of the intima. Therefore it is essential to investigate the interaction between arterial layers and the role of each layer in the uptake of the macromolecules and development of atherosclerosis. Using a multi-layer model and solving a proper set of governing equations and boundary conditions can result in an accurate description of dynamics and distribution of macromolecules across the arterial wall.

Indeed, this model provides the most realistic description of the arterial anatomy. However, it requires a large number of parameters to characterize the transport properties of each layer. There are limitations in the direct measurement of the properties of tissues (specifically human tissues). For this reason, many efforts have been devoted to the characterization of these parameters. A number of investigations have been performed based on the assumption that the arterial wall layers are porous structures with physical properties which can be identified using the pore theory [73,79,57,58,61,3,72,76,77].

Karner and Perktold [76] investigated the influence of endothelial damage and blood pressure on albumin accumulation in the arterial wall. They assumed a fully developed stationary blood flow and calculated the filtration velocity in the wall layers using Darcy's law. Using a numerical model they coupled the mass transport processes in the arterial lumen and in the various layers of the arterial wall: endothelium, intima, IEL and media. They used a stationary convection diffusion equation to model the luminal mass transport. The transport in the porous intima and media was modeled applying the volume-averaged stationary convection–diffusion-reaction equation. In their analysis, the transport processes in the lumen, intima, and media were coupled by the flux across the endothelium and IEL based on using the Staverman–Kedem–Katchalsky equations. These equations are given as

$$V = \frac{K'}{\mu}(\Delta p - \sigma_d \Delta \pi) \tag{22}$$

$$N''_S = D'_e \Delta c + (1 - \sigma_f) V \bar{c} \tag{23}$$

where V is the velocity vector of bulk flow across the membrane, N''_S the absolute molar flux of the solute across the membrane, Δp the pressure differential across the membrane, $\Delta \pi$ the corresponding osmotic pressure differential, Δc the solute concentration differential, K' the permeability per unit length, D'_e the effective diffusivity per unit length, $\bar{c}$ the mean solute concentration over the membrane, and σ_f and σ_d are the Staverman filtration and osmotic reflection (which account for the selective permeability of biological membranes to certain solutes) coefficients, respectively. The Staverman–Kedem–Katchalsky membrane equations are usually used to model the transport processes in the endothelium and IEL in the previous multi-layer models. However, the traditional Staverman–Kedem–Katchalsky equations have at least two substantial disadvantages: it is derived based on the existence of pseudo-steady state condition, which is in conflict with the real physiological conditions existing within both endothelium and IEL and it ignores the boundary effects on the flow across the membrane, which is not valid when the boundaries of the porous membrane have to be accounted for [2].

Karner and Perktold [76] demonstrated a high resistance of the healthy endothelium to macromolecule exchange between blood and the arterial wall. They also discussed that reduced resistance of an injured endothelium causes an increased mass flux into the wall which results in higher concentration levels within the wall. Their results showed that the effect of the blood pressure on the wall concentration level is different for healthy and injured endothelium. In the case of a healthy endothelium a blood pressure increase caused a decrease of the intimal concentration and an increase of the media concentration, whereas in the case of an injured endothelium an increased blood pressure resulted in higher concentration levels within the intima and media.

In their mathematical and numerical study of LDL transport within the arteries, Prosi et al. [63] employed a multi-layer model composed of endothelium, intima, IEL, and media. They solved Navier–Stokes equation and the advection–diffusion equation to obtain the flow and concentration fields within the lumen. For the transport processes within the arterial layers, they used Darcy's law coupled with the species equation given by

$$\frac{\partial\langle c\rangle}{\partial t}+\nabla\cdot\left(-D_{\mathrm{e}}\nabla\langle c\rangle+\frac{\gamma_{\mathrm{h}}}{\varepsilon}\langle V\rangle\langle c\rangle\right)+k\langle c\rangle=0 \tag{24}$$

where γ_{h} is the hindrance coefficient for the transport of species. They considered available data on the LDL concentration profiles [80,81,55,59] and computed for each model a set of parameters that best fit these measurements. To fulfill this task, they applied the basic equations governing the mass transport through the arterial wall, reinterpreting these equations by means of an electric analogy. Through the analogy, they derived a set of algebraic equations to determine the unknown physical parameters with respect to available measured data.

Yang and Vafai [2] developed a new fundamental four-layer model for the description of the mass transport in the arterial wall coupled with the mass transport in the arterial lumen. In their study, the arterial wall layers, i.e. endothelium, intima, IEL and media, were considered as macroscopically homogeneous porous media. A schematic of their model is presented in Fig. 4. They obtained the luminal flow field and species distribution by solving the unsteady Navier–Stokes and advection–diffusion equations. They mathematically modeled LDL transport across their four-layer model using proper types of the volume averaged porous media equations, with the Staverman filtration and osmotic reflection coefficients employed to account for selective permeability of each porous layer to certain solutes. They used the following equations for the endothelium and IEL layers

$$\frac{\rho_{\mathrm{f}}}{\varepsilon}\frac{\partial\langle V\rangle}{\partial t}+\frac{\mu}{K}\langle V\rangle=-\nabla\langle P\rangle^{f}+R_{\mathrm{u}}T\sigma_{\mathrm{d}}\nabla c+\mu_{\mathrm{e}}\nabla^{2}\langle V\rangle \tag{25}$$

$$\frac{\partial\langle c\rangle}{\partial t}+(1-\sigma_{\mathrm{f}})\langle V\rangle\cdot\nabla\langle c\rangle=D_{\mathrm{e}}\nabla^{2}\langle c\rangle \tag{26}$$

where R_{u} and T are the universal gas constant and the absolute temperature of the medium, respectively. For the intima and media, the osmotic effect in the transport modeling is not included. This is due to the fact the maximum osmotic pressure gradient is far below the hydraulic pressure gradient. As such, they employed the following set of governing equations for the intima and media layers

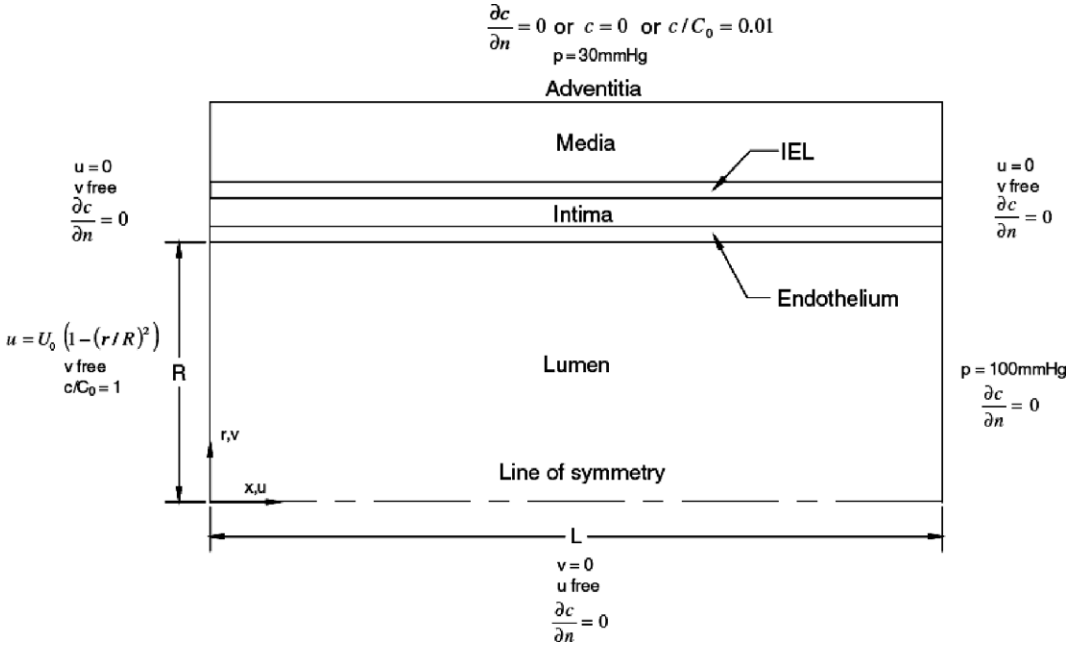

Fig. 4. Multi-layer model of an arterial wall presented by Yang and Vafai [2].

$$\frac{\rho_f}{\varepsilon}\frac{\partial\langle V\rangle}{\partial t}+\frac{\mu}{K}\langle V\rangle=-\nabla\langle P\rangle^f+\mu_e\nabla^2\langle V\rangle \tag{27}$$

$$\frac{\partial\langle c\rangle}{\partial t}+(1-\sigma_f)\langle V\rangle\cdot\nabla\langle c\rangle=D_e\nabla^2\langle c\rangle+k\langle c\rangle \tag{28}$$

where k is the effective volumetric first order reaction rate coefficient. To investigate the effects of media–adventitia boundary condition on the LDL distribution across the arterial layers, Yang and Vafai [2] used three types of concentration boundary conditions at the media–adventitia interface

$$\frac{c}{C_0}=0,\quad \frac{c}{C_0}=0.01,\quad \frac{\partial c}{\partial n}=0 \tag{29}$$

where C_0 is the reference value for the species concentration. At the interfaces between lumen, endothelium, intima, IEL, and media the following concentration boundary condition was employed

$$\left[(1-\sigma_f)Vc-D_e\frac{\partial c}{\partial n}\right]_+=\left[(1-\sigma_f)Vc-D_e\frac{\partial c}{\partial n}\right]_- \tag{30}$$

They also studied the effects of hypertension on the LDL transport within the arterial wall to identify possible factors that might be responsible for enhanced arterial wall uptake of LDL under hypertensive conditions. They concluded that a pressure-induced increase of endothelial diffusive permeability, plus pressure-driven convective flow, is mainly responsible for the enhanced LDL uptake at a higher transmural pressure, which might explain increased atherosclerosis susceptibility in the presence of hypertension. They also stated that hypertension greatly increases the transmural filtration and concentration polarization at the lumen/endothelium interface. Fig. 5 shows the influence of transmural pressure and endothelial diffusivity on LDL distribution across the arterial layers. It is shown that the LDL uptake within different layers is largely affected by the transmural pressure and endothelial diffusivity.

They also reported that the filtration velocity and LDL concentration profile in the media layer is dependent on different types of boundary conditions, as shown in Fig. 6. The LDL concentration in the endothelium, intima, and IEL show no dependence on the type of boundary condition at the adventitia. For example, they found that the traction-free boundary condition leads to a significant jump in the filtration velocity profile near the outlet. Yang and Vafai [2] also found that pulsatile flows play a minor role in the LDL transport within the arterial wall when a straight axisymmetric geometry is considered.

In another study, Ai and Vafai [78] utilized a similar four-layer-wall model to study the macromolecule transport in a stenosed arterial wall. They employed the fundamental equations of porous media to characterize the properties associated with the wall layers. Starting from these governing equations and the well established experimental data of the wall permeability and concentration profile in the media, they determined the parameters associated with each layer. Ai and Vafai [78] then utilized these parameters in their model and investigated the effects of hypertension in both normal and stenosed arteries. Their model gave good estimation of velocity and species distributions in the lumen and within the arterial wall. They found that the maximum shear rate appears before the throat while the velocity vector reaches its maximum value slightly after the throat. In addition, they established that the wall concentration is substantially enhanced near the region of stenosis and approaches its unperturbed value shortly after the stenosis.

Table 1 represents the types of governing equations used in arterial transport modeling. Different types of boundary conditions utilized in the arterial transport modeling are presented in Table 2.

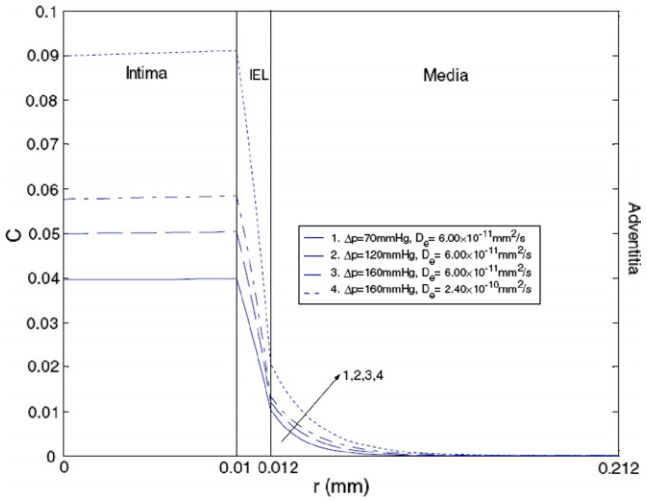

Fig. 5. The influence of transmural pressure and endothelial diffusivity on LDL distribution across the arterial layers [2].

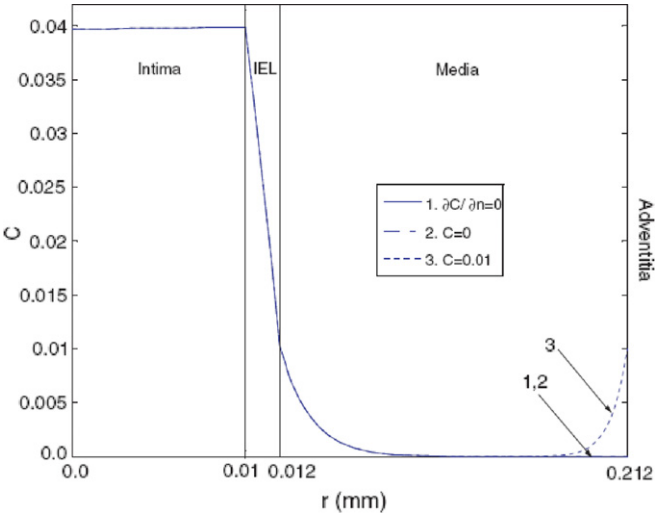

Fig. 6. Effects of different concentration boundary conditions at the media adventitia interface on the LDL distribution across the arterial layers [2].

Table 1
Summary of the governing equations used in arterial transport modeling

	Fluid flow governing equations	Species transport governing equations
Lumen	Navier–Stokes equation [64–67,76,63,2,78]: $\rho\frac{\partial V}{\partial t}+\rho V\cdot\nabla V=-\nabla p+\mu\nabla^2 V$	Advection–diffusion equation [64–67,76,63,2,78]: $\frac{\partial c}{\partial t}+V\cdot\nabla c=D\nabla^2 c$
	Navier–Stokes equation incorporating Womersley parameter [69]: $\alpha^2\frac{\partial u}{\partial t}+Re\,u\cdot\nabla u+Re_1\nabla p-\nabla^2 u=0$	Advection–diffusion equation incorporating Womersley parameter [69]: $\alpha^2\frac{\partial c}{\partial t}+Re\,u\cdot\nabla c-\frac{1}{Sc}\nabla^2 c=0$
Arterial wall	Darcy equation [76,63,70]: $\vec{V}=-\frac{\overline{\overline{\mathrm{K}}}}{\mu}.\nabla p$	Advection–diffusion equation [70,76]: $\frac{\partial c}{\partial t}+V\cdot\nabla c=D\nabla^2 c$
	Brinkman equation: $\frac{\mu}{K}.\langle V\rangle=-\nabla\langle p\rangle^f+\mu_e\nabla^2\langle V\rangle$	Advection–diffusion equation incorporating Womersley parameter [68,69]: $\alpha^2\frac{\partial c}{\partial t}+Re\,u\cdot\nabla c-\frac{1}{Sc}\nabla^2 c=0$
	Expanded Brinkman equation incorporating Womersley parameter [68,69]: $\alpha^2\frac{\partial u}{\partial t}+Re\,u\cdot\nabla u+Re_1\nabla p-\nabla^2 u+\frac{R^2}{K}u=0$	Advection–diffusion-reaction equation [76]: $\frac{\partial c}{\partial t}+V\cdot\nabla c=D\nabla^2 c+\dot{\omega}$
	Volume averaged generalized equation: $\frac{\rho_f}{\varepsilon}\left[\frac{\partial\langle V\rangle}{\partial t}+\langle(V\cdot\nabla)V\rangle\right]=-\nabla\langle P\rangle^f+\frac{\mu}{\varepsilon}\nabla^2\langle V\rangle-\frac{\mu}{K}\langle V\rangle-\frac{\rho_f F\varepsilon}{K^{1/2}}[\langle V\rangle\cdot\langle V\rangle]J$	Kedem–Katchalsky membrane species transport equation [76,63,2,78]: $N_S''=D_e'\Delta c+(1-\sigma_f)V\bar{c}$
	Kedem–Katchalsky membrane transport equation [76,63,2,78]: $V=\frac{K'}{\mu}(\Delta p-\sigma_d\Delta\pi)$	Advection–diffusion-reaction equation incorporating a hindrance coefficient [63]: $\frac{\partial\langle c\rangle}{\partial t}+\nabla\cdot\left(-D_e\nabla\langle c\rangle+\frac{\gamma}{\varepsilon}\langle V\rangle\langle c\rangle\right)+k\langle c\rangle=0$
	Volume-averaged momentum equation accounting for Staverman osmotic reflection coefficient for endothelium and IEL [2,78]: $\frac{\rho_f}{\varepsilon}\frac{\partial\langle V\rangle}{\partial t}+\frac{\mu}{K}\langle V\rangle=-\nabla\langle P\rangle^f+R_u T\sigma_d\nabla c+\mu'\nabla^2\langle V\rangle$	Volume-averaged species transport equation accounting Staverman filtration coefficient: for endothelium and IEL [2,78]: $\frac{\partial\langle c\rangle}{\partial t}+(1-\sigma_f)\langle V\rangle\cdot\nabla\langle c\rangle=D_e\nabla\langle c\rangle^2$; for Intima and Media [2,78]: $\frac{\partial\langle c\rangle}{\partial t}+(1-\sigma_f)\langle V\rangle\cdot\nabla\langle c\rangle=D_e\nabla\langle c\rangle^2+k\langle c\rangle$

Table 2
Summary of the boundary conditions used in arterial transport modeling

Model	Interface/boundary	Boundary condition	
		Fluid flow	Species transport
Wall-free [64–67]	Luminal side boundaries	Constant filtration velocity [64–67]: $V_{\text{filt}} = \text{const.}$	Net transmural flux [64–67]: $V_{\text{w}} c_{\text{w}} - D\left.\frac{\partial c}{\partial n}\right\|_{\text{w}} = J_{\text{s}}$
Homogeneous wall [68–70]	Inner interface (lumen–wall)	Constant filtration velocity [68–70]: $V_{\text{filt}} = \text{const.}$	Net transmural flux [68–70]: $V_{\text{w}} c_{\text{w}} - D\left.\frac{\partial c}{\partial n}\right\|_{\text{w}} = J_{\text{s}}$
	Outer interface (wall-adventitia)	Zero variation in normal direction [68–70]: $\left.\frac{\partial V}{\partial n}\right\|_{\text{w}} = 0$	Zero variation in normal direction [68–70]: $\left.\frac{\partial c}{\partial n}\right\|_{\text{w}} = 0$
Multi-layer wall [76,63,2,78]	Lumen–endothelium interface Endothelium–intima interface Intima–IEL interface IEL–media interface	Zero variation in normal direction [76,63,2,78]: $\left.\frac{\partial V}{\partial n}\right\|_{\text{w}} = 0$	Net transmural flux [76,63,2,78]: $\left[(1-\sigma_{\text{f}})Vc - D_{\text{e}}\frac{\partial c}{\partial n}\right]_{+} = \left[(1-\sigma_{\text{f}})Vc - D_{\text{e}}\frac{\partial c}{\partial n}\right]_{-}$
	Media–adventitia	Homogeneous Neumann in normal direction [76,63,2,78]: $\left.\frac{\partial V}{\partial n}\right\|_{\text{w}} = 0$	Homogeneous Dirichlet [76,63,2,78]: $\frac{c}{C_0} = 0$ Non-homogeneous Dirichlet [63,2,78]: $\frac{c}{C_0} = 0.01$ Homogeneous Neumann [63,2,78]: $\frac{\partial c}{\partial n} = 0$

6. Conclusions

Transport processes are present in various aspects of biological sciences. Interactions involving fluid mechanics, heat transfer, and mass transport in biology and medicine are fundamental in understanding the causes of diseases and in the development of new prophylactic, diagnostic, and therapeutic procedures. Nearly all the human tissues are categorized as porous media; thus transport process in porous media plays a substantial role in biology. The application of transport through porous media in biological and biomedical sciences is an ever-expanding field of research. It has been utilized to study numerous pertinent transport processes including diffusion-weighted magnetic resonance imaging (DW-MRI), drug delivery, and transport within tissues and their role in initiation and development of cardiovascular diseases. Over the past few decades, various research works have been performed; each providing additional understanding of transport processes involved in the onset and development of cardiovascular diseases such as atherosclerosis. One of the fields of study, which has substantially benefited from porous media modeling, is transport within the arteries.

There are three major challenges in modeling of the arterial transport. These are accurate description of the artery, proper set of governing equations, and appropriate choice of boundary conditions. Over the years, different arterial transport models have been proposed as a result of a trade-off between accuracy and feasibility/cost. Three major models used in the arterial transport modeling were analyzed. Out of these three, the multi-layer model describes the arterial anatomy most accurately. In this model, the arterial wall is composed of four porous layers with different physiological characteristics. The multi-layer model requires a number of transport parameters (properties) for each layer and in return provides an accurate profile for macromolecule distribution across the arterial wall, illuminating the role and behavior of each porous layer in transport of macromolecules across the arterial wall.

Another important factor in the accurate modeling of arterial transport is the use of a proper set of governing equations that take into account the dominant processes involved in the transport phenomenon. Various types of governing equations and boundary conditions have been used in each arterial transport model. Transport within lumen is obtained by solving the Navier–Stokes equation along with the species advection–diffusion equation. Due to their relative simplicity, Darcy and Brinkman models have often been employed to solve for the momentum transport within the porous layers. However, in addition to an oversimplification, these models do not account for the osmotic pressure, as discussed by Yang and Vafai [2], and Ai and Vafai [78]. In a number of studies, species transport is represented via an advection–diffusion equation. This equation does not include the change in the species concentration due to biochemical reactions. In addition, it does not incorporate the selective permeability of each porous layer to certain solutes. As described by Yang and Vafai [2], and Ai and Vafai [78], the Staverman filtration and osmotic reflection coefficients must be included to account for the selective rejection of species by the endothelium and IEL porous membranes as well as the effects of osmotic pressure.

Although advancing rapidly, the study of biological transport phenomena is faced with a number of challenges. Some aspects of transport through porous media in relation to biological tissues have not been properly addressed and more fundamental research is warranted. For instance, to date, more accurate measurement of the transport properties of biological tissues, such as porosity, permeability, and diffusivity remains one of the challenges in the modeling of transport processes within biological tissues. Applicability and validity of animal-based experimental results to human diseases and lack of human-based results pose another challenge. While a great majority of studies are devoted to cases of normal arteries and stenosed arteries, the transition between the two stages, that is the initiation and growth of the stenosis in time, has not been modeled.

References

[1] American Heart Association Heart Disease and Stroke Statistics-2007. Update. American Heart Association, Dallas, TX, 2007.

[2] N. Yang, K. Vafai, Modeling of low-density lipoprotein (LDL) transport in the artery-effects of hypertension, Int. J. Heat Mass Transfer 49 (2006) 850–867.

[3] Z.J. Huang, J.M. Tarbell, Numerical simulation of mass transfer in porous media of blood vessel walls, Am. J. Physiol. 273 (1997) H464–H477.

[4] R.P. Vito, S.A. Dixon, Blood vessel constitutive models —1995–2002, Annu. Rev. Biomed. Eng. 5 (2003) 413–439.

[5] A. Quarteroni, M. Tuveri, A. Veneziani, Computational vascular fluid dynamics: problems, models, and methods, Comput. Visual. Sci. 2 (2000) 163–197.

[6] D.N. Ku, Blood flow in arteries, Ann. Rev. Fluid Mech. 29 (1997) 399–434.

[7] G.D.O. Lowe, J.C. Barbenel, Plasma and blood viscosity, in: G.D.O. Lowe (Ed.), Clinical Blood Rheology, vol. 1, CRC Press, Boca Raton, FL, 1988.

[8] S. Chien, Biophysical behavior of red cells in suspension, in: D.M. Surgenor (Ed.), Red Blood Cell, vol. 3, Academic Press, New York, 1975.

[9] O.K. Baskurt, H.J. Meiselman, Blood rheology and hemodynamics, Semin. Thromb. Hemost. 29 (2003) 435–450.

[10] R.L. Replogle, H.J. Meiselman, E.W. Merrill, Clinical implications of blood rheology studies, Circulation 36 (1967) 148.

[11] N.A. Casson, Flow Equation for the Pigment Oil Suspensions of the Printing Ink Type. Reology of Disperse Systems, Pergamon Press, NewYork, 1959, pp. 84–102.

[12] D. Quemada, Rheology of concentrated disperse systems II. A model for non-newtonian shear viscosity in steady flows, Rheol. Acta 17 (1978) 632–642.

[13] L. Ai, K. Vafai, An investigation of Stokes' second problem for non-Newtonian fluids, Numer. Heat Transfer A 47 (2005) 955–980.

[14] M.W. Rampling, Red cell aggregation and yield stress, in: G.D.O. Lowe (Ed.), Clinical Blood Rheology, vol. 1, CRC Press, Boca Ration, FL, 1988, pp. 65–86.

[15] R. Nerem, Hemodynamics and the vascular endothelium, ASME J. Biomech. Eng. 115 (1993) 510–514.

[16] R. Nerem, Vascular fluid mechanics, arterial wall and atherosclerosis, ASME J. Biomech. Eng. 114 (1992) 274–282.

[17] S. Glagov, C. Zarins, D.P. Giddens, D.N. Ku, Hemodynamics and atherosclerosis: insights and perspectives gained from studies of human arteries, Arch. Pathol. Lab. Med. 112 (1988) 1018–1031.

[18] H.F. Younis, M.R. Kaazempur-Mofrad, R.C. Chan, A.G. Isasi, D.P. Hinton, A.H. Chau, L.A. Kim, R.D. Kamm, Hemodynamics and wall mechanics in human carotid bifurcation and its consequences for atherogenesis: investigation of inter-individual variation, Biomech. Model Mechanobiol. 3 (2004) 17–32.

[19] W.W. Nichols, M.F. O'Rourke, McDonald's Blood Flow in Arteries, Edward Arnold, London, 1990.

[20] C. Zarins, D. Giddens, B. Bharadvaj, V. Sottiurai, R. Mabon, S. Glagov, Carotid bifurcation atherosclerosis: quantitative correlation of plaque localization with flow velocity profiles and wall shear stress, Circ. Res. 53 (1983) 502–514.

[21] A.M. Malek, S.L. Alper, S. Izumo, Hemodynamic shear stress and its role in atherosclerosis, JAMA 282 (1999) 2035–2042.

[22] S.A. Berger, L.-D. Jou, Flows in stenotic vessels, Annu. Rev. Fluid Mech. 32 (2000) 347–382.

[23] Z. Lou, W.J. Yang, Biofluid dynamics at arterial bifurcations, Crit. Rev. Biomed. Eng. 19 (1992) 455–493.

[24] D.L. Fry, Acute vascular endothelial changes associated with increased blood velocity gradients, Circ. Res. 22 (1968) 165–197.

[25] D.L. Fry, Certain histological and chemical responses of the vascular interface to acutely induced mechanical stress in the aorta of the dog, Circ. Res. 24 (1969) 93–108.

[26] R. Rayman, R.G. Kratky, M. Roach, Steady flow visualization in a rigid canine aortic cast, J. Biomech. 18 (1985) 863–875.

[27] C.G. Caro, J.M. Fitz-Gerald, R.C. Schroter, Atheroma and arterial wall shear observations correlation and proposal of a shear dependent mass transfer mechanism for atherogenesis, Proc. Roy. Soc. Lond. B 177 (1971) 109–159.

[28] K. Kandarpa, N. Davids, Analysis of the fluid dynamic effects on atherogenesis at branching sites, J. Biomech. 9 (1976) 735–741.

[29] T. Karino, M. Motomiya, H. Goldsmith, Flow patterns at the major T-junctions of the dog descending aorta, J. Biomech. 23 (1990) 537–548.

[30] D.N. Ku, D.P. Giddens, C.K. Zarins, S. Glagov, Pulsatile flow and atherosclerosis in the human carotid bifurcation – positive correlation between plaque location and low and oscillating shear stress, Arteriosclerosis 5 (1985) 293–302.

[31] G. Helmlinger, R.V. Geiger, S. Schreck, R.M. Nerem, Effects of pulsatile flow on cultured vascular endothelial cell morphology, J. Biomech. Eng. 113 (1991) 123–131.

[32] J.E. Moore Jr., D.N. Ku, C.K. Zarins, S. Glagov, Pulsatile flow visualization in the abdominal aorta under differing physiologic

conditions: implications for increased susceptibility to atherosclerosis, J. Biomech. Eng. 114 (1992) 391–397.
[33] E.M. Pedersen, A.P. Yoganathan, X.P. Lefebvre, Pulsatile flow visualization in a model of the human abdominal aorta and aortic bifurcation, J. Biomech. 25 (1992) 935–944.
[34] D.P. Giddens, C.K. Zarins, S. Glagov, The role of fluid mechanics in the localization and detection of atherosclerosis, J. Biomech. Eng. 115 (1993) 588–594.
[35] P.F. Davies, A. Remuzzi, E.J. Gordon, C.F. Dewey Jr., M.A. Gimbrone Jr., Turbulent fluid shear stress induces vascular endothelial cell turnover in vitro, Proc. Natl. Acad. Sci. USA 83 (1986) 2114–2117.
[36] N. DePaola, M.A. Gimbrone Jr., P.F. Davies, C.F. Dewey Jr., Vascular endothelium responds to fluid shear stress gradients, Arterioscler. Thromb. 12 (1992) 1254–1257.
[37] M. Lei, C. Kleinstreuer, G.A. Truskey, Numerical investigation and prediction of atherogenic sites in branching arteries, J. Biomech. Eng. 117 (1995) 350–357.
[38] M. Lei, C. Kleinstreuer, G.A. Truskey, A focal stress-dependent mass transfer mechanism for atherogenesis in branching arteries, Med. Eng. Phys. 18 (1996) 326–332.
[39] C. Kleinstreuer, M. Lei, J.P. Archie, Flow input waveform effects on the temporal and spatial wall shear stress gradients in a femoral graft-artery connector, J. Biomech. Eng. 118 (1996) 506–510.
[40] C. Kleinstreuer, J.R. Buchanan Jr., M. Lei, G.A. Truskey, Computational analysis of particle-hemodynamics and prediction of the onset of arterial diseases, in: C.T. Leondes (Ed.), Biomechanics Systems Techniques and Applications, Gordon & Breach, New York, 1998.
[41] M.H. Friedman, G.M. Hutchins, C.B. Bargeron, O.J. Deters, F.F. Mark, Correlation of human arterial morphology with hemodynamic measurements in arterial casts, J. Biomech. Eng. 103 (1981) 204–207.
[42] J.M. Huyghe, Y. Schröder, F.P.T. Baaijens, Bioengineering: the future of poromechanics, in: 17th ASCE Engineering Mechanics Conference, University of Delaware, Newark, DE, June 13–16, 2004.
[43] A.-R.A. Khaled, K. Vafai, The role of porous media on modeling flow and heat transfer in biological tissues, Int. J. Heat Mass Transfer 46 (2003) 4989–5003.
[44] J.M. Huyghe, T. Arts, D.H. Van Campen, R.S. Reneman, Porous medium finite element model of the beating left ventricle, Am. J. Physiol. 262 (1992) H1256–H1267.
[45] S.L. Bulter, S.S. Kohles, R.J. Thielke, C. Chen, R. Vanderby, Interstitial fluid flow in tendons or ligaments: a porous medium finite element simulation, Med. Biol. Eng. Comput. 35 (1997) 742–746.
[46] X.X. Lei, W.Y. Wu, G.B. Wen, J.G. Chen, Mass transport in solid tumors (I) – fluid dynamics, Appl. Math. Mech. Eng. Ed. 19 (1998) 1025–1032.
[47] J.W. Baish, P.A. Netti, R.K. Jain, Transmural coupling of fluid flow in microcirculatory network and interstitium in tumors, Microvasc. Res. 53 (1997) 128–141.
[48] J.M. Huyghe, D.H. Van Campen, Finite deformation theory of hierarchically arranged porous solids – II. Constitutive behavior, Int. J. Eng. Sci. 33 (1995) 1873–1886.
[49] W.J. Vankan, J.M. Huyghe, M.R. Drost, J.D. Janssen, A. Huson, A finite element mixture model for hierarchical porous media, Int. J. Numer. Meth. Eng. 40 (1997) 193–210.
[50] K. Vafai, C.L. Tien, Boundary and inertia effects on flow and heat transfer in porous media, Int. J. Heat Mass Transfer 24 (1981) 195–203.
[51] K. Vafai, A. Bejan, W.J. Minkowycz, K. Khanafer, A Critical Synthesis of Pertinent Models for Turbulent Transport through Porous Media. Handbook of Numerical Heat Transfer, second ed., Wiley, Hoboken, NJ, 2004 (Chapter 12).
[52] J. Bear, Y. Bachmat, Introduction to Modeling of Transport Phenomena in Porous Media, Kluwer Academic, Dordrecht, 1990.
[53] R.K. Dash, K.N. Mehta, G. Jayaraman, Casson fluid flow in a pipe filled with a homogeneous porous medium, Int. J. Eng. Sci. 34 (1996) 1145–1156.
[54] S. Tada, J.M. Tarbell, Interstitial flow through the internal elastic lamina affects shear stress on arterial smooth muscle cells, Am. J. Physiol. 278 (2000) H1589–H1597.
[55] J. Tarbell, M. Lever, C. Caro, The effect of varying albumin concentration and hydrostatic pressure on hydraulic conductivity of the rabbit common carotid artery, Microvasc. Res. 35 (1988) 204–220.
[56] E.D. Morris, G.M. Saidel 3rd, Chisolm, optimal design of experiments to estimate LDL transport parameters in arterial wall, Am. J. Physiol. 261 (1991) H929–H949.
[57] H. Jo, R.O. Dull, T. Hollis, J. Tarbell, Endothelial albumin permeability is shear dependent, time dependent, and reversible, Am. J. Physiol. 260 (1991) H1992–H1996.
[58] D. Wang, J. Tarbell, Modeling interstitial flow through arterial media, ASME J. Biomech. Eng. 117 (1995) 358–363.
[59] R. Dull, H. Jo, H. Still, T. Hollis, J. Tarbell, The effect of varying albumin concentration and hydrostatic pressure on hydraulic conductivity and albumin permeability of cultured endothelial monolayers, Microvasc. Res. 41 (1991) 390–407.
[60] Y. Huang, D. Rumschitzki, S. Chien, S. Weinbaum, A fiber matrix model for the growth of macromolecular leakage spots in the arterial intima, ASME J. Biomech. Eng. 116 (1994) 430–445.
[61] Y. Huang, Y. Rumschizki, D. Chien, S. Weinbaum, A fiber matrix model for the filtration through fenestral pores in a compressible arterial intima, Am. J. Physiol. 272 (1997) H2023–H2039.
[62] G. Truskey, W. Roberts, R. Herrmann, R. Malinauskas, Measurement of endothelial permeability to ^{125}I-low density lipoproteins in rabbit arteries by use of En face preparations, Circ. Res. 7 (1992) 883–897.
[63] M. Prosi, P. Zunino, K. Perktold, A. Quarteroni, Mathematical and numerical models for transfer of low-density lipoproteins through the arterial walls: a new methodology for the model set up with applications to the study of disturbed luminal flow, J. Biomech. 38 (2005) 903–917.
[64] L. Back, J. Radbill, D. Crawford, Analysis of oxygen transport from pulsatile, viscous blood flow to diseased coronary artery of man, J. Biomech. 10 (1977) 763–774.
[65] G. Rappitsch, K. Perktold, Pulsatile albumin transport in large arteries: a numerical simulation study, ASME J. Biomech. Eng. 118 (1996) 511–519.
[66] G. Rappitsch, K. Perktold, E. Pernkopf, Numerical modeling of shear-dependent mass transfer in large arteries, Int. J. Numer. Meth. Fluids 25 (1997) 847–857.
[67] S. Wada, T. Karino, Theoretical prediction of low-density lipoproteins concentration at the luminal surface of an artery with a multiple bend, Annu. Biomed. Eng. 30 (2002) 778–791.
[68] C.R. Ethier, J.A. Moore, Oxygen mass transfer calculations in large arteries, ASME J. Biomech. Eng. 119 (1997) 469–475.
[69] D. Stangeby, C. Ethier, Coupled computational analysis of arterial ldl transport-effects of hypertension, Comput. Meth. Biomech. Biomed. Eng. 5 (2002) 233–241.
[70] N. Sun, N.B. Wood, A.D. Hughes, S.A.M. Thom, X.Y. Xu, Fluid-wall modelling of mass transfer in an axisymmetric stenosis: effects of shear-dependent transport properties, Ann. Biomed. Eng. 34 (2006) 1119–1128.
[71] O. Kedem, A. Katchalsky, Thermodynamic analysis of the permeability of biological membranes to non-electrolytes, Biochim. Biophys. Acta 27 (1958) 229–246.
[72] W. Shyy, S. Thakur, H. Ouyang, J. Liu, E. Blosch, Computational Techniques for Complex Transport Phenomena, Cambridge University Press, Cambridge, 1997.
[73] F.E. Curry, Mechanics and thermodynamics of transcapillary exchange, in: E.M. Renkin (Ed.), Handbook of Physiology, vol. IV, American Physiological Society, Bethesda, MD, 1984.
[74] D. Fry, Mathematical models of arterial transmural transport, Am. J. Physiol. 248 (1985) H240–H263.
[75] D. Fry, Mass transport, atherogenesis, and risk, Arteriosclerosis 7 (1987) 88–100.

[76] G. Karner, K. Perktold, Effect of endothelial injury and increased blood pressure on albumin accumulation in the arterial wall: a numerical study, J. Biomech. 33 (2000) 709–715.
[77] G. Karner, K. Perktold, H. Zehentner, Mass transport in large arteries and through the arterial wall, in: P. Verdonck, K. Perktold (Eds.), Intra and Extracorporeal Cardiovascular Fluid Dynamics, WIT-Press-Computational Mechanics Publications, Southampton, Boston, 2000.
[78] L. Ai, K. Vafai, A coupling model for macromolecule transport in a stenosed arterial wall, Int. J. Heat Mass Transfer 49 (2006) 1568–1591.
[79] W.M. Deen, Hindered transport of large molecules in liquid filled pores, AIChE J. 33 (1987) 1409–1425.
[80] G. Meyer, R. Merval, A. Tedgui, Effects of pressure stretch and convection on low-density-lipoprotein and albumin uptake in the rabbit aortic wall, Circ. Res. 79 (1996) 532–540.
[81] R. Bratzler, G. Chisolm, C. Colton, K. Smith, R. Lees, The distribution of labeled low-density lipoproteins across the rabbit thoracic aorta in vivo, Atherosclerosis 28 (1977) 289–307.